Biochimica et Biophysica Acta, 1062 (1991) 133–141

ADONIS 000527369100107M

BBAMEM 75147

Lipid polymorphism as observed by cryo-electron microscopy

Peter M. Frederik [1], Koert N.J. Burger [2], Marc C.A. Stuart [1] and Arie J. Verkleij [3]

[1] *EM Unit, Department of Pathology, University of Limburg, Maastricht (The Netherlands),* [2] *Institute of Molecular Biology and Medical Biotechnology, University of Utrecht, Utrecht (The Netherlands) and* [3] *Department of Molecular Cell Biology, University of Utrecht, Utrecht (The Netherlands)*

(Received 9 July 1990)

Key words: Lipid polymorphism; Cryo-electron microscopy; Electron microscopy

Lipid polymorphism was studied with the aim to gain more insight in bilayer to non-bilayer phase transitions, with particular emphasis on the development of cubic structures on one hand and inverted hexagonal structures on the other hand. Thin vitrified films prepared from aqueous lipid suspensions were used in this study. The entire hydrated contents of these films can be visualized in their two-dimensional projection by cryo-electron microscopy. As the starting material, unilamellar vesicles were prepared from mixtures of dioleoylphosphatidylethanolamine, dioleoylphosphatidylcholine and cholesterol. By heating of the suspension, vesicle fusion (Frederik et al. (1989) Biochim. Biophys. Acta 979, 275–278) and lipid polymorphism was induced. From these suspensions thin films were prepared at various temperatures, and vitrified for low temperature observation. In a parallel series of experiments samples were fast-frozen for freeze-fracture analysis. In vitrified thin films bilayer structures were often observed in coexistence with an inverted hexagonal structure. The bilayer areas were frequently of a complex structure because multiple contacts between stacked membranes were found. These contact points were variable in size and shape and usually had the form of a diabolo (when viewed side-on) giving the impression of a bilayer contact with an aqueous channel. This structure is compatible with the interlamellar attachment site (ILA) proposed by Siegel ((1986) Biophys. J. 49, 1155–1170). In some specimens ILA's seemed to merge into arrays. After thermal cycling of the suspension, arrays of packed globules were observed, which are likely the result of close packing of ILA's. The arrays probably represent a cubic structure. A comparison of freeze-fracture replicas and vitrified thin films indicated that both techniques may provide valuable structural information on lipid polymorphism. Most of the lipidic particles observed by freeze-fracturing probably correspond to the ILA's (fractured around their waist region) as observed in vitrified thin films. The results obtained with vitrified thin films were interpreted in relation to the principles of thin-film formation. Finally, we speculate that lipid structures occurring close to each other in space may represent a developmental series of structures occurring successively in time.

Introduction

Membrane fusion is a key event in cell biology. Exocytosis, endocytosis and infection by enveloped virusses are common examples of cellular events that require fusion of membranes. At some stage during membrane fusion the equilibrium bilayer configuration of membrane lipids has to be temporarily abandoned. A significant proportion of the lipids present in all biomembranes reveals a tendency to form inverted non-bilayer lipid structures such as the hexagonal H_{II} phase, and model membrane studies have clearly shown that these lipids play a facilitating if not essential role in membrane fusion [1,2]. However, the actual intermediates in bilayer to non-bilayer lipid phase transitions and membrane fusion have remained ill-defined [3].

The ultrastructural description of fusion events and lipid phase transitions is largery based on freeze-fracture studies (for review, see Verkleij [4]) and started with the description of lipidic particles as putative fusion intermediates [2]. Both these freeze-fracture studies and recent theoretical models of lipid phase behaviour

Correspondence: P.M. Frederik EM-unit, Department of Pathology/BMC, University of Limburg, P.O. Box 616, 6200 MD Maastricht, The Netherlands.

and membrane fusion [5–7] support the idea of an inverted lipid micelle (or 'inverted micellar intermediate', IMI, [8]) acting as a transient intermediate both in membrane fusion (joining stage) and in bilayer to inverted non-bilayer lipid phase transitions. The lifetime of IMI's is predicted to be extremely short (0.1–1 ms). The IMI's either collapse and the original situation of two separate bilayers is restored, or they coalesce to form precursors of the hexagonal H_{II} phase. Finally, IMI's may spontaneously convert into a fusion pore with a small aqueous channel (fission). These early fission stages (interlamellar attachment sites, ILA's) are predicted to be metastable structures that may form (depending on a shape factor of the molecules involved, [6,9]) at or slightly below the $L\alpha \rightarrow H_{II}$ phase transition temperature. ILA's have a relatively long lifetime as compared to IMI's. Whereas IMI's represent the fusion stage at which two membranes become continuous, the ILA's represent the 'fission' stage at which an aqueous connection is established between the contents of two vesicles. Furthermore, a bicontinuous cubic phase is thought to arise when ILA's assemble into closely-packed long-lived arrays [7,10]. In this paper we will describe the ultrastructure of a number of pure lipid systems that undergo an $L\alpha$ to H_{II} phase transition. Since membrane fusion and bilayer to inverted non-bilayer lipid phase transitions probably share common intermediates, an improved morphological characterization of bilayer to non-bilayer lipid phase transitions may provide valuable information on the mechanism of membrane fusion. Until recently, only freeze-fracture electron microscopy could be used to study the ultrastructure of hydrated membranes. In the last few years, the study of hydrated objects by cryo-electron microscopy made a great stride forward due to the work of Dubochet and co-workers (for review, see Ref. 11). It was soon acknowledged that cryo-electron microscopy is ideally suited to study artificial membranes [12–15]. The advantage of cryo-electron microscopy in this respect is the possibility to visualize the entire contents of a hydrated thin film (thinner than 200 nm) without a need for chemical pretreatment or replication. Whereas thin-sections and freeze-fracture electron microscopy offer a limited view (a cross-section or a fracture plane) of the ultrastructure of a sample, cryo-electron microscopy visualizes the whole sample in its two-dimensional projection (also see Discussion). Therefore, the exact spatial relationship between coexisting lipid phases (e.g., $L\alpha$, isotropic and H_{II}) can be determined. In addition, the combination of fast-freezing (vitrification) and cryo-electron microscopy allows for the observation of short-lived fusion intermediates [13].

With these advantages in mind we used cryo-electron microscopy to investigate lipid phase behaviour. In order to be able to relate the data obtained by cryo-electron microscopy to data already available from freeze-fracture studies [4], cryo-electron microscopy and freeze-fracture electron microscopy were performed in parallel, on the same lipid suspensions. The lipid system chosen was a mixture of dioleoylphosphatidylethanolamine (DOPE), cholesterol and dioleoylphosphatidylcholine (DOPC), in which fusion can be triggered by a rise in temperature. Recently we described the ultrastructure of thin films prepared from this lipid mixture while searching for early fusion intermediates [13]. In the course of our investigations we noticed that complicated structures form when fusogenic conditions are maintained for longer time-periods. The ultrastructure is complex, as will be described in this paper, because coexisting states of lipids were present within a single area of observation. The vitrification of thin films combined with cryo-electron microscopy is thus used to reveal the spatial relationship between these coexisting structural states. It became tempting to interprete adjoining structures, which are successive in space, as stages succeeding each other in time when lipid transforms under the influence of a change in temperature.

The data presented show that vitrified thin films are particularly well suited for the study of lipid polymorphism; lamellar, hexagonal and cubic phases are imaged in their spatial relationship probably together with transitional intermediates. Cryo-electron microscopy allowed for the identification of one of the proposed type II fusion intermediates, the interlamellar attachment site (ILA). A comparison with freeze-fracture experiments performed in parallel showed a correlation in size and shape of lipidic particles (FF) with interlamellar attachments (cryo EM). This correlation has some implications for the interpretation of freeze-fracture images.

The preparation of a thin film from a lipid suspension may affect the lipid structures suspended in the film. This should be taken into consideration when interpreting the results obtained by cryo-electron microscopy.

Materials and Methods

Preparation of phospholipid suspensions

The phospholipids dioleoylphosphatidylethanolamine (DOPE, P 0510) and dioleoylphosphatidylcholine (DOPC, P 1013) were obtained from Sigma. Cholesterol was obtained from Baker. Dry mixed films of DOPE, cholesterol and DOPC were prepared in a molar ratio of 3 : 2 : 1, 3 : 1 : 2 or 3 : 1 : 3 by evaporating the solvent (chloroform) under a stream of dry nitrogen gas. The mixed films were redissolved in methanol dried under a stream of dry nitrogen gas, and finally hydrated in Tris-HCl buffer (10 mM Tris, 150 mM NaCl, pH 7.4). The final lipid concentration was 12 mM. From this suspension unilamellar vesicles were prepared by repeated sonication (10 s pulse, 10 s pause) at 4°C until a

clear suspension was obtained, or by extrusion through polycarbonate filters (0.2 μm pore size; Nuclepore) at 4°C using the extruder described by Hope et al. [16]. The suspensions thus obtained were used 'directly' for thin film formation (control) or were heated to 50–70°C until macroscopically visible aggregates were formed; and a thin film was formed after thorough vortexing of the suspension.

Thin film preparation and cryo-electron microscopy

A thin aqueous film was formed by dipping and withdrawing a bare specimen grid from the suspension. The grids had a fine (700 mesh) honeycomb pattern of bars and were only 3–4 μm thick. After withdrawal from the phospholipid suspension the grid was blotted against filter paper. Thin films were vitrified within one second after their formation by plunging the grid into ethane cooled to its melting point by liquid nitrogen. A gravity-powered guillotine was used to guide the tweezers holding the grid into the ethane [17]. The temperature at which the thin films were formed and from which vitrification was initiated, was usually room temperature with a few exceptions (e.g., Figs. 1 b, c d). Vitrification from an elevated temperature (50–70°C) was performed by placing the vitrification equipment and all solutions in an incubator at high humidity [18]. The grids with the vitrified films were either mounted in a Gatan cryoholder (model 626) or a Philips cryoholder (model PW 6599/00). After transfer of the holder to the microscope particular attention was paid to the thermal equilibration of the holder. The shields covering the specimen were only opened after 30 min to prevent contamination of the specimen by a transient rise in the vapour pressure of water [19,20] and to prevent thermal drift of the cryoholder. Micrographs were taken at 100 kV and a specimen temperature of −170°C (Gatan cryoholder) or −190°C (Philips cryoholder). In order to obtain enough contrast, advantage was taken of the increase in contrast at large defocus values (see Refs. 11 and 21, for review). Defocus values of 2–6 μm were employed to optimally resolve structural details of 4–6 nm in size.

Freeze-fracture electron microscopy

Samples (1 μl) of the lipid suspension were sandwiched between two copper platelets (Balzers, Liechtenstein).

The sandwich samples were fast frozen by plunging them into liquid propane (−190°C), using a plunge freezing device (KF 80, Reichert Jung, Wien, Austria). No cryoprotectants were used. Fracturing and replication were carried out using standard procedures. The replicas were stripped and cleaned with dilute chromic/sulfuric acid and distilled water according to Costello et al. [22]. Micrographs were taken at 80–100 kV using a Philips CM 10 or CM 12 electron microscope.

Results and Discussion

Cryo-electron microscopy and thin film formation

All starting suspensions of unilamellar vesicles had a similar appearance when vitrified in a thin film and observed by cryo-electron microscopy (not shown). A thin rim of the film is usually found devoid of vesicles [12, 23] and in a thicker part of the film vesicles are found more or less sorted by size. At first approximation it may seem that the images of vitrified thin films are representative of the structures in the bulk phase. However, for the interpretation of images it is essential to consider the events involved in the formation of a thin film spanning the holes in a 'bare' specimen grid (or a holey carbon grid). This thin film, which spontaneously forms after blotting, is composed of a thin aqueous layer bordered by two monolayers of phospholipid molecules one at each air/water interface. Such a thin aqueous film will further thin spontaneously, initially driven by gravity and capillary forces until the London-van der Waals attractive forces between the apposing monolayers come into play. In thinner films (< 100 nm) this attraction will dominate (and eventually accelerate) further thinning until the attractive forces come into balance with the short range electrostatic and hydration repulsive forces. The result of this thinning is the expulsion of water from the thin central part of the film towards the thicker annulus (the 'Gibb's border') near the grid bars. As thinning radially spreads out from the center of a film, material in suspension is concentrated and sorted by size, and eventually material becomes trapped between the biconcave monolayers at the rim of the film [12,13]. Material in the film can eventually be forced to arrange in a sheet-like fashion. The effects of film thinning can be observed in many of the thin films from which cryo EM images are presented. It should be emphasized that the draining of thin films (< 100 nm) proceeds as a consequence of intermolecular forces and therefore also progresses in an atmosphere with a high environmental humidity. Furthermore it should be noted that the formation of the two monolayers at the air water interface requires recruitement of material from the suspension. In our study in the order of 20% of the lipid initially trapped in a thin film between the grid bars may participate in the formation of monolayers at the two airwater interfaces. This figure was calculated on the assumption that the average film thickness after blotting is 3 μm (the thickness of the grid) and contains a 12 mM lipid suspension, taking 0.45 nm^2 as the mean molecular area (an area found for phospholipid/cholesterol molecules in a 1 : 1 ratio at an air/water interface with a surface tension of 30 $mN\,m^{-1}$). This calculation should be interpreted in a qualitative sense; monolayer formation at the air/water interfaces depletes the suspension to a certain extend but it leaves enough lipid in suspension

to study lipid polymorphism by cryo-electron microscopy.

Lipid polymorphism as observed in vitrified thin films

Upon heating, the unilamellar vesicles of the starting suspension are destabilized. Fusion results in the formation of larger bilayer structures and type II non-bilayer lipid structures. Often a lace-work of interwoven membranes is found (e.g., Fig. 1a), and even within one micrograph, bilayer, H_{II} and 'isotropic', i.e., highly curved in all directions (these types of structures would be expected to result in an isotropic ^{31}P-NMR signal), structures are found in coexistence (e.g., Fig. 2b). The lipid structures observed can be divided into two groups; structures which are characteristic of the transition from the Lα to the isotropic/cubic state (Fig. 1) and structures characteristic of the transition from the Lα to the hexagonal H_{II} phase (Fig. 2). Of course, this subdivision of lipid structures implies interpretation of the morphological data, and is only a simplified description of these data.

The large bilayer structures formed upon heating show many membrane interconnections. These interconnections have the shape and dimensions as proposed for one of the putative membrane fusion intermediates, namely the interlamellar attachment site (ILA; see Introduction). Cryo-electron microscopy identifies these ILA's as structures measuring some 11 nm at their waist connecting membranes 10–15 nm apart. Many micrographs (e.g., Fig. 1a) show a local variation in the frequency of occurrence of these ILA's. Areas apparently composed of undisturbed bilayers are found intermingled with rows of ILA's. Areas with ILA's present as separate entities may merge into areas crowded with ILA's; many areas are found in which ILA's seem to have locally condensed into regular arrays. Some micrographs (e.g., Fig. 1a) show all the different types of ILA organization and strongly suggest that an increase in the degree of organization of ILA's reflects the successive stages in the development of a cubic structure; a bicontinuous cubic state in which ILA's function as the building blocks [5,10].

The orientation of an ILA with respect to the plane of observation determines the shape of its 2D-projection as observed by cryo-electron microscopy. In Fig. 1b a remarkebly large proportion of ILA's is observed side-on having the shape of a diabolo. We assume that this preferential orientation of ILA's is due to an alignment of lipid structures that may occur during thin film formation (see later). When ILA's are viewed head-on they should appear as ring-shaped profiles. Indeed, the arrays of circular profiles as found in, e.g., Fig. 1c are most likely representative of closely packed ILA's viewed head-on. It should be noted that considerable variation is observed in the diameter of these circular profiles even on a single micrograph. In Fig. 1c, e.g., the diameter varies between 10 and 15 nm. This micrograph once more suggests, in agreement with contemporary theory, that a bicontinuous cubic lipid state is formed from stacked bilayers according to the schematic representation in Fig. 1f; ILA's form between bilayer sheets, and in the end an isotropic or cubic arrangement of ILA's originates. The close packing of ILA's (e.g., Fig. 1d) strongly suggests the development of a cubic structure. However, it should be noted that long range order is not (yet?) established in these specimens. This is evidenced by the presence of only first order diffraction spots upon optical diffraction of the micrographs (data not shown). Therefore, we cannot assign a (cubic) space group to the arrangement of packes ILA's as observed in vitrified thin films. However, on a theoretical basis [5,6,10] a further ordering would be expected to result in a cubic structure. Finally, ILA's formed at the edge of stacked membranes (cf. Fig. 1f) are tilted with respect to the plane of observation and elliptic profiles are observed (e.g., Fig. 1c; also see Ref. 24).

Fig. 1. Lipid polymorphism in DOPE/cholesterol/DOPC mixtures showing structures related to isotropic/cubic states. (a) Vitrified thin films were prepared from a suspension of DOPE/cholesterol/DOPC (molar ratio 3:2:1) and heated to 60°C. Film formation and vitrification were initiated at room temperature. Areas with smooth bilayers are found intermingled with areas displaying multiple contacts between bilayers (ILA's viewed side-on, arrow heads). In some areas circular profiles are found, probably representing ILA's viewed head-on, that have organized into a cubic arrangement (asterisk). (b) A vitrified thin film was prepared from a suspension of DOPE/cholesterol/DOPC (molar ratio 3:1:2) and heated to 50°C. Thin-film formation and vitrification were carried out at 50°C in a controlled environment. ILA's (viewed side-on) are found organized into rows (e.g., between the arrow heads), or have seemingly condensed into larger arrays (asterisk). (c) A vitrified thin film was prepared from a suspension of DOPE/cholesterol/DOPC (molar ratio 3:1:3) and heated to 60°C. Thin-film formation and vitrification were carried out at 60°C. Stacked bilayers with many ILA's are found in coexistence with smooth bilayers. In the stacked bilayers most ILA's are observed head-on (arrow). When ILA's have formed at the edge of stacked membranes, they are titled with respect to the plane of observation and elliptic profiles are observed (arrow heads) (also see Ref. 24). Note the increase in order towards the center of the micrograph. (d) A vitrified thin film prepared from a suspension of DOPE/cholesterol/DOPC (molar ratio 3:1:3). The suspension was repeatedly heated to 70°C and cooled to 7°C before thin films were prepared (and vitrified) at 70°C. A cubic arrangement of ILA's viewed head-on is observed in coexistence with a vesicle. Long range order is lacking since optical diffraction of the micrograph only revealed first order spots (not shown). (e) Freeze-fracture replica from a suspension of DOPE/cholesterol/DOPC (molar ratio 3:1:3), heated to 60°C, cooled to room temperature and subsequently fast frozen. Lipidic particles of variable size and shape show up, occasionally assembled into clusters (arrow head). (f) Tentative scheme illustrating the development of a cubic state from multiple ILA's formed between stacked bilayers. A concentric arrangement of bilayers (top) may give rise to the same type of structure. ILA's are drawn side-on (cf. Fig. 1b). Micrographs are printed at the same final magnification, bar represents 200 nm.

A detailed description of the various projected views of ILA's is presented in a recent report by Siegel et al. [24] on vitrified thin films prepared from *N*-monomethylated DOPE and observed by cryo-electron microscopy. Siegel et al. [24] used an experimental approach comparable to the approach used in our study except for the choice of lipid. The micrographs presented by Siegel et al. [24] as well as the description of

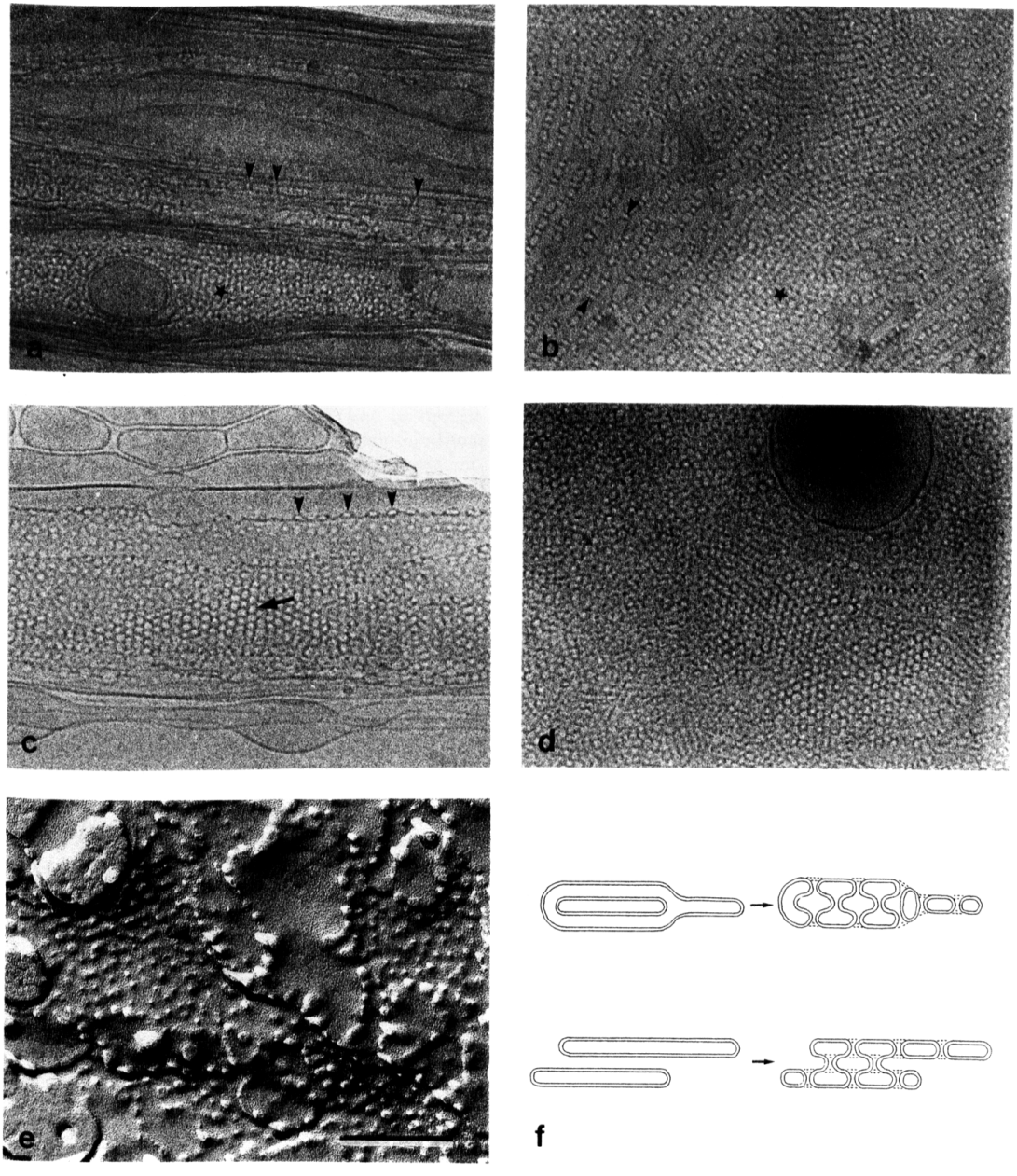

the structural intermediates involved in the formation of isotropic or cubic lipid states, are confirmed by the observations presented in this paper. The striking similarities in the polymorphic behaviour of methylated DOPE and DOPE/DOPC/ cholesterol mixtures can been explained on a theoretical basis. Both lipid systems have a similar intrinsic radius of curvature [25] and a similar $L\alpha/H_{II}$ headgroup ratio, i.e., the ratio between the surface areas of the phospholipid headgroups in the $L\alpha$ and the H_{II} phase [5–8]. These theories are based on a number of physicochemical data and are also supported by morphological evidence from freeze-fracture studies [26]. Further morphological evidence on this similarity in the polymorphic behaviour between methylated DOPE and DOPE/DOPC/ cholesterol mixtures is now provided by the study of vitrified thin films (c.f. Ref. 24 and this report). The ultrastructure of the lipid suspensions is strongly influenced by their thermal history. For instance, the micrograph presented in Fig. 1d was obtained by repeated cycling around the $L\alpha \rightarrow H_{II}$ phase transition temperature. This procedure favours the formation of isotropic/cubic structures [27].

If on the other hand a sample is heated without thermal cycling, the hexagonal H_{II} phase predominates, as illustrated in Fig. 2. Tubes of about 20 nm in diameter were found running parallel with tubes having a diameter of 8 nm (Fig. 2b). The diameter of the latter tubes is in the same order as the diameter reported for H_{II} cylinders in freeze-fracture studies of the same lipid mixture (8.6 nm; [4,28] confirmed in this study, see Fig. 2d; also see Ref. 29). The small tubes most likely represent an H_{II} phase. The diameter of the 20 nm tubes virtually excludes them being H_{II} cylinders; these tubes are interpreted as being bilayer tubes. The spatial relationship between these bilayer tubes and the H_{II} cylinders is very suggestive of a developmental relationship. Interestingly, in Fig. 2a a repeat distance of 13 nm is found, suggesting the presence of large H_{II} cylinders with a diameter intermediate between that of the small H_{II} cylinders and the bilayer tubes. It should also be

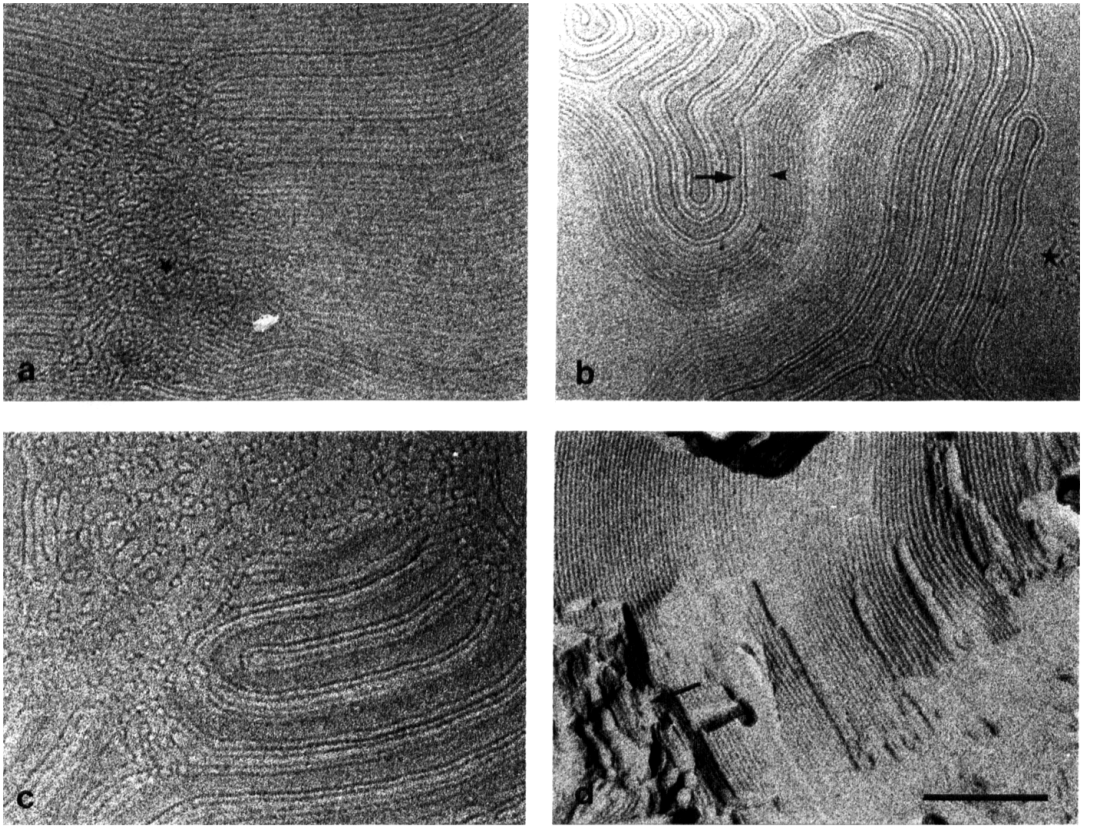

noted that the H_{II} cylinders and bilayer tubes are arranged close to, and in a plane parallel to the interfaces (Figs. 2a, b, c). The orientation of the bilayer tubes and H_{II} cylinders may be influenced by thin film formation. Lipid material may be forced into a planar orientation during draining of the thin film (see first part of Results and Discussion). On the other hand densitometry [12] showed that thin films were often much thicker than the diameter of the lipid structures residing in the film arranged in a sheet-like fashion (e.g., in Fig. 2c film thickness is 180 ± 20 nm, bilayer tubes ⌀20 nm); as a consequence other lipid structures could sometimes be observed running for instance underneath the parallel arranged structures at the upper interface (not shown). In these cases the planar orientation of lipid structures may be a surface-related phenomenon. It should be realized that restructuring of lipid (e.g., $H_{II} \rightarrow L\alpha$) at or close to the interface may have played a role in some of the thin films from which images are presented. In this context it is important to remark that vitrification can be virtually ruled out as a cause of temperature induced changes in lipid structure. The preservation of thermotropic lipid phases could be demonstrated using vesicles of dipalmitoylphosphatidylcholine; vesicles were either smooth ($L\alpha$) or rippled ($P_{\beta'}$) depending on the temperature at which thin films were vitrified, above or below te gel to liquid-crystalline phase transition temperature (42°C) [18]. The fact that temperature-sensitive lipid phases can be faithfully preserved by vitrification underlines the usefulness of the thin film approach for the study of (temperature induced) lipid polymorphism.

Cryo-electron microscopy versus freeze-fracturing

In order to be able relate the data obtained by cryo-electron microscopy to data already available from freeze-fracture studies on lipid polymorphism, cryo-electron microscopy and freeze-fracture electron microscopy were performed in parallel on the same lipid suspensions. Micrographs are therefore presented at the same final magnification. Some interpretation of the images was involved in the selection of the pictures (isotropic/cubic and H_{II}) because of the polymorphic nature of the lipid structures. Upon comparing of the micrographs, the question arises whether the lipidic particles as defined by freeze-fracture analysis are to be interpreted as fractures through the ILA's observed by cryo-electron microscopy. Lipidic particles are a group of structures associated with membrane fusion/fission [4] and the description that follows is largely based on freeze-fracture analysis of suspensions of DOPE/DOPC/cholesterol (molar ratio 3:1:2). Large particles of variable size and shape are thought to represent the adhesion stage preceeding membrane fusion. Well-defined semispherical particles (⌀9.5 nm), may represent the joining stage with an inverted lipid micelle (IMI) sandwiched in between the two interacting membranes. The vulcano-like protrusions with a central depression (larger than 20 nm ⌀) or a flat top are thought to represent the fission stage of membrane fusion, i.e., the stage at which an aqueous connection has formed between two originally separated compartments. It should be noted cleary, that lipidic particles have been described as a family of related structures of various sizes and shapes, and it should be noted that the ILA's as observed by cryo-electron microscopy appear to be heterogeneous in size and shape as well. Based on their size, the vulcano-like protrusions with a central depression or a flat top may well correspond to ILA's fractured slightly above or below their waist region. In fact, it cannot be excluded that even the well-defined semispherical particles thought to represent the joining stage of membrane fusion (IMI, see before), also correspond to post-fusion structures, i.e., small ILA's fractured through their waists. In conclusion both cryo-electron microscopy and freeze-fracture electron microscopy seem to positively identify one of the proposed type II fusion intermediates, the ILA; but the structural intermediate present at the crucial stage of membrane fusion, the stage at which two membranes join, still remains elusive. Although contemporary theory supports the involvement of an inverted lipid micelle, only morphological techniques offering high temporal and spatial resolution may in the end proof the actual presence of an IMI during membrane fusion. Biophysical measurements [10] and theoretical considerations [7] disfavour the presence of IMI's in (meta)stable lipid phases as those described in this report, but do not exclude

Fig. 2. Lipid polymorphism in DOPE/cholesterol/DOPC mixtures with structures related to the inverted hexagonal (H_{II}) phase. (a) A vitrified thin film was prepared from a suspension of DOPE/cholesterol/DOPC (molar ratio 3:2:1) kept at 4°C. Film formation and vitrification were done at room temperature. Putative H_{II} cylinders (repeat distance 13–14 nm) terminate in a disordered fine meshwork (asterisk). (b) A vitrified thin film prepared from a suspension of DOPE/cholesterol/DOPC (molar ratio 3:2:2) kept at room temperature. Film formation and vitrification were initiated at room temperature. Bilayer (arrrow), H_{II} (arrow head) and isotropic (asterisk) structures are found in coexistence. A wavy bundle of H_{II} cylinders (arrow head) is found in coexistence with larger tubes (arrow). The walls of these tubes are probably lined by a lipid bilayer (also see Fig. 2c). (c) A vitrified thin film prepared from a suspension of DOPE/cholesterol/DOPC (molar ratio 3:1:1) heated to 40°C. Film formation and vitrification were initiated at room temperature. Bilayer tubes (as found in Fig. 2b) are now bordered by areas with extensive ILA formation (compare with Fig. 1b). (d) Freeze-fracture replica from a suspension of DOPE/cholesterol/DOPC (molar ratio 3:2:1) heated to 60°C, cooled to room temperature and subsequently fast frozen. H_{II} cylinders are found in coexistence with bilayer areas (arrow). Micrographs are printed at the same final magnification, bar represents 200 nm.

their presence during membrane fusion and lipid phase transitions (lamellar to hexagonal H_{II} phase). A definitive answer with respect to the existence of the IMI can possibly be given when more cryo-electron microscopic data on synchronized fusion events become available (e.g., by using a temperature jump or a pH drop and synchronized vitrification). At present, these experiments are a technological challenge [30] and the number of observations on early fusion events in thin films is too limited [13] for final conclusions to be drawn.

In freeze-fracturing as well as in thin-film formation lipid structures are often observed in a preferred orientation. In freeze-fracturing the fracture plane takes a preferential course through the mechanically weakest parts of the specimen (e.g., splitting bilayers into halves, or fracturing through the highly curvatured waist region of ILA's). In vitrified thin films interface formation and spontaneous film thinning (as discussed before) may result in a preferred orientation of lipid structures. The cubic structures (Fig. 1) and the inverted hexagonal cylinders (Fig. 2) are examples of structures observed in a preferred orientation in vitrified thin films. In freeze-fracture replicas this is less obvious. Information from these two cryotechniques is thus complementary, freeze-fracturing revealing the interior of fractured membranes or the membrane surface (after etching) whereas in cryo-electron microscopy the whole vitrified sample is visualized in its projection at a high resolution (potentially).

Conclusions and prospects

Cryo-electron microscopy of vitrified thin films revealed the various structures that develop around the $L\alpha \rightarrow H_{II}$ phase transition temperature. Bilayer structures including interlamellar attachments (ILA's), and complex structures (e.g., isotropic, cubic) that are formed after multiple ILA formation, could be observed in vitrified thin films, as well as inverted hexagonal cylinders. When interpreting cryo-electron microscopic data obtained on vitrified thin films, it turned out to be important to consider the process of thin film formation. Two events in the formation and thinning of aqueous films may affect lipid structure. The first event is the formation of interfacial layers and we speculated that this may guide the arrangement of lipid structures. The second event that may affect lipid structure occurs later when the aqueous film becomes thinner. During thinning the interfacial layers approach each other and water is expelled from the thin central parts towards the thicker periphery. Lipid in the suspension may also become concentrated into sheets arranged parallel to the interfaces. A low water content may favour ILA formation and it is important to realize that, in principle, ILA's may form prior to but also during thin-film formation. Lipid structures may also be forced to arrange in a sheet-like fashion parallel to the interfaces. We have suggested that film thinning may result in a preferred orientation of the captured structures as evidenced by the high proportion of interlamellar attachments that is viewed head-on. In conclusion an aqueous thin film is not simply a sample representing the bulk suspension, but a sample in which the arrangement of its components is to some extend governed by the process of film thinning and the behaviour of material at the air/water interfaces. The further characteristics of vitrified thin films, a 'through-vision' of the entire hydrated contents, make the study of lipid polymorphism by cryo-electron microscopy meaningful. Comparing data from vitrified thin films with the data obtained from parallel experiments using freeze-fracture replication indicated that these techniques provide complementary data. Both techniques can be used to reveal the structures involved in lipid polymorphism. The comparison between vitrified thin films and freeze-fracture replicas showed that lipidic particles such as the well-defined spherical particle and the vulcano-like protrusions fall within the size range of ILA's as observed by cryo-electron microscopy. Further data are required on (synchronized) early fusion events in thin films before any firm conclusions can be drawn on the existence of the still largely hypothetical membrane joining intermediate, the inverted lipid micelle. The use of vitrified thin films in this respect is one of the challenging goals of cryo-electron microscopy requiring high spatial resolution as well as high resolution on a time-scale. In addition vitrified films can be used for the study of protein mediated membrane fusion, such as the pH induced fusion of influenza virus with liposomes [31]. Also in this application we expect that cryo-electron microscopy, using the fast process of vitrification (10^{-5} s) in conjunction with the high spatial resolution of the transmission electron microscope, may disclose structural details of local-point fusion that were previously hidden by a lack in time and/or spatial resolution.

References

1 Cullis, P.R. and Hope, M.J. (1978) Nature 271, 672–674.
2 Verkleij, A.J., Mombers, C., Leunissen-Bijvelt, J. and Ververgaert P.H.J.T. (1979) Nature 279, 162–163.
3 Burger, K.N.J. and Verkleij, A.J. (1990) Experientia 46, 631–644.
4 Verkleij, A.J. (1984) Biochim. Biophys. Acta 779, 43–63.
5 Siegel, D.P. (1986) Biophys. J. 49, 1155–1170.
6 Siegel, D.P. (1986) Biophys. J. 79, 1171–1183.
7 Siegel, D.P. (1986) Chem. Phys. Lipids 42, 279–301.
8 Siegel, D.P. (1984) Biophys. J. 45, 399–420.
9 Kirk, G.L., Gruner, S.M. and Stein, D.L. (1984) Biochemistry 23, 1093–1102.
10 Lindblom, G. and Rilfors, L. (1989) Biochim. Biophys. Acta 988, 221–256.
11 Dubochet, J., Adrian, M., Chang, J.-J., Lepault, J. and McDowall, A. (1987) in Cryotechniques in Biological Electron Microscopy (Steinbrecht, R.A. and Zierold, K., eds.), Chapter 5, pp. 114–131, Springer Verlag, Berlin-Heidelberg.

12 Frederik, P.M., Stuart, M.C.A., Bomans, P.H.H. and Busing, W.M. (1989) J. Microsc. 153, 81–92.
13 Frederik, P.M., Stuart, M.C.A. and Verkleij, A.J. (1989) Biochim. Biophys. Acta 979, 275–278.
14 Lepault, J., Pattus., F. and Martin, N. (1985) Biochim. Biophys. Acta 820, 315–318.
15 Talmon, Y. (1986) Colloids Surfaces 19, 237–248.
16 Hope, M.J., Bally, M.b., Webb, G. and Cullis, P.R. (1985) Biochim. Biophys. Acta 812, 55–65.
17 Dubochet, J., Lepault, J., Freeman, R., Berriman, J.A. and Homo, J.-C. (1982) J. Microsc. 128, 219–237.
18 Frederik, P.M., Stuart, M.C.A., Bomans, P.H.H., Busing, W.M., Burger, K.N.J. and Verkleij, A.J. (1990) J. Microsc., in press.
19 Frederik, P.M. and Busing, W.M. (1986) J. Microsc. 144, 215–222.
20 Trinick, J., Cooper, J., Seymour, J. and Engelmann, E.H. (1986) J. Microsc. 141, 349–360.
21 Dubochet, J., Adrian, M., Chang, J.-J., Homo J.-C., Lepault, J., McDowall, A.W. and Schulz, P. (1988) Quart. Rev. Biophys. 21, 129–228.
22 Costello, M.J., Fetter, R. and Höchli, M (1982) J. Microsc. 125, 125–136.
23 Frederik, P.M., Stuart, M.C.A, Schrijvers, A.H.G.J. and Bomans, P.H.H. (1989) Scanning Microsc. Suppl. 3, 277–284.
24 Siegel, D.P., Burns, J.L., Chestnut, M.H. and Talmon, Y. (1989) Biophys. J. 56, 161–169.
25 Gruner, S.M. (1985) Proc. Natl. Acad. Sci. USA 82, 3665–3669.
26 Gagne, J., Stamatatos, L., Diacovo, Hui, S.W., Yeagle, P.L. and Silvius, J.R. (1985) Biochemistry 24, 4400–4408.
27 Shyamsunder, E., Gruner, S.M., Tate, M.W., Turner, D.C., So, P.T.C. and Tilcock, C.P.S. (1988) Biochemistry 27, 2332–2336.
28 Van Venetië, R. and Verkleij, A.J. (1981) Biochim. Biophys. Acta 600, 625–635.
29 Gruner, S.M., Tate, M.W., Kirk, G.L., So, P.T.C., Turner, D.C., Keane, D.T., Tilcock, C.P.S. and Cullis, P.R. (1988) Biochemistry 27, 2853–2866.
30 Talmon, Y., Burns, J.L., Chestnut, M.H. and Siegel, D.P. (1990) J. Electron Microsc. Techn. 14, 6–12.
31 Burger, K.N.J., Knoll, G., Frederik, P.M. and Verkleij, A.J. (1990) in Dynamics and Biogenesis of Membranes (Op den Kamp, J.A.F., ed.), NATO ASI Series, Vol. H 40, pp. 185–196, Springer Verlag, Berlin-Heidelberg.